

# Thermodynamics of the quark-gluon plasma at finite chemical potential: color path integral Monte Carlo results

V.S. Filinov<sup>1</sup> \*, M. Bonitz<sup>2</sup>, Y.B. Ivanov<sup>3</sup>, M. Ilgenfritz<sup>4</sup>, and V.E. Fortov<sup>1</sup>

<sup>1</sup> Joint Institute for High Temperatures, Russian Academy of Sciences, Izhorskaya 13, bd. 2, 125412 Moscow, Russia

<sup>2</sup> Institute for Theoretical Physics and Astrophysics, Christian Albrechts University Kiel, Leibnizstrasse 15, D-24098 Kiel, Germany

<sup>3</sup> Russian Research Center “Kurchatov Institute”, Kurchatov Sq. 1, 123182 Moscow, Russia

<sup>4</sup> Joint Institute for Nuclear Research, Joliot-Curie str., 6, Dubna, Moscow Region, 141980, Russia

Received XXXX, revised XXXX, accepted XXXX

Published online XXXX

**Key words** strongly coupled plasma, quark gluon plasma

**PACS** 12.38Mh, 31.15.Qg, 51.20.+d, 52.27Gr

Based on the constituent quasiparticle model of the quark-gluon plasma (QGP), color quantum path-integral Monte-Carlo (PIMC) calculations of the thermodynamic properties of the QGP are performed. We extend our previous zero chemical potential simulations to the QGP at finite baryon chemical potential. The results indicate that color PIMC can be applied not only above the QCD critical temperature  $T_c$  but also below  $T_c$ . Besides reproducing the lattice equation of state our approach yields also valuable additional insight into the internal structure of the QGP, via the pair distribution functions of the various quasiparticles. In particular, the pair distribution function of gluons reflects the existence of gluon-gluon bound states at low temperatures and  $\mu = 175$  MeV, i.e. glueballs, while meson-like bound states are not found.

Copyright line will be provided by the publisher

## 1 Basics of the QGP model and comparison with PIMC for plasmas

Strongly correlated charged particle systems have attracted growing interest over the recent three decades in many fields. This includes laser compressed plasmas [1], ions in traps, dusty plasmas [2] or dense plasmas in planet cores. For the theoretical description of dense quantum plasmas path integral Monte Carlo (PIMC) simulations have proved particularly successful, e.g. [3, 4]. A few years ago experiments at the Relativistic Heavy-Ion Collider (RHIC) at Brookhaven National Laboratory [5] and at the Large Hadron Collider (LHC) at CERN [6] have produced an unconfined quark–gluon plasma (QGP) which turned out to behave as a nonideal liquid [5, 7]. Although equilibrium properties of the strongly QGP are successfully computed using lattice QCD [5, 8, 9], these simulations are very time consuming and not easy to interpret. Also, they fail, e.g. at large quark chemical potential. Based on the above mentioned experience with PIMC simulations of strongly correlated Coulomb systems it is, therefore, tempting to make these methods available also for the description of the QGP. We have developed such “color PIMC” simulations in recent years, e.g. [10–12] focusing on zero baryon chemical potential. Here we extend these simulations to the important case of finite chemical potential. In the following we briefly discuss the model [13] and present first results for the thermodynamic properties.

To start with we provide a comparison of an (“electromagnetic”) electron-ion plasma and a quark gluon plasma, see Table 1, since this provides the basis to understand the main physical ingredients required for realistic color PIMC simulations. Although QCD was constructed in analogy to quantum electrodynamics there exist fundamental differences. While Coulomb interacting charges are mapped on fermions (or bosons) whose interaction is mediated by (usually weakly interacting) photons the situation in QCD is different. Here also the field particles (gluons) providing the interaction between fermions (quarks and antiquarks) are, in general,

\* Corresponding author E-mail: vladimir.filinov@mail.ru,

**Table 1** Comparison of an Electromagnetic plasmas and the QGP model simulated in this paper. **Comments and notations:**  $T$ : temperature,  $\mu$ : chemical potential,  $r_{ab}$ : distance between particles a and b, QP: quasiparticles. <sup>a</sup> Only intrinsic, no orbital quantum numbers are listed. <sup>b</sup> defined by the kinetic energy operator.

	Electromagnetic plasma	Semiclassical SU(3) quark-gluon plasma
Basic particles/QP	electrons, ions (i) or holes (h)	quarks, antiquarks, gluons
Quantum numbers <sup>a</sup>	spin	spin, flavor, color
Renormalization	none (plasmas), QP in solids	QP
Masses	$m_e \ll m_i$ or QP masses $m_e \sim m_h$	comparable QP masses, $m_\alpha = m_\alpha(T, \mu)$
Charge	fixed scalar electrical charge $q_\alpha$	SU(3) Wong vector color charge variables $Q_\alpha$
Coupling constant	fixed value, $\alpha = 1/137$	state and distatnt dependent, $\alpha(T, \mu, r_{ab})$
Potential energy	non-relativistic Coulomb potential $V_{ab} \sim q_a q_b / r_{ab}$	non-relativistic color Coulomb potential $V_{ab} \sim \alpha(T, \mu, r_{ab}) Q_a \bullet Q_b / r_{ab}$ $Q_a \bullet Q_b$ scalar product of 8D vectors
Kinetic energy	non-relativistic	relativistic
Path integral partition function <sup>b</sup>	non-relativistic Gaussian measure	relativistic Bessel and SU(3) group Haar measures

strongly interacting. It is, therefore, advantageous to consider not bare quarks, antiquarks and gluons but quasiparticles by absorbing the “hard modes” into the quasiparticles whereas the soft modes are incorporated into an effective color Coulomb interaction [13].

The basic assumptions of our model are similar to those of Ref. [14]:

- I.:** Quasiparticles masses ( $m$ ) are of order or higher than the mean kinetic energy per particle. This assumption is based on the analysis of QCD lattice data [15–17]. For instance, at zero net-baryon density it amounts to  $m \sim T$ , where  $T$  is a temperature.
- II.:** In view of I., the interparticle interaction is dominated by a color-electric Coulomb potential.
- III.:** Since the color representations are large, the color operators are substituted by their average values [by Wong’s classical color vectors, i.e. eight-dimensional (8D) vectors in SU(3)] with the quadratic and cubic Casimir conditions [18].
- IV.:** We consider the 3-flavor (‘up’, ‘down’ and ‘strange’) quark model assuming equal quark masses. The gluon (quasiparticle) mass is allowed to be different (heavier) from that of the quarks.

Thus, this model requires the following three input quantities as a function of temperature ( $T$ ) and quark chemical potential ( $\mu_q$ ): the quasiparticle masses, for quarks  $m_q$  and gluons  $m_g$ , and the coupling constant  $g^2$ , or  $\alpha_s = g^2/4\pi$ . These input quantities should be deduced from lattice QCD data or from an appropriate model simulating these data.

The applicability of such an approach was discussed in Refs. [14, 19] in detail. It has been established that hard modes (in terms of *hard thermal loop* approximation [20–22]) behave like quasiparticles. Therefore, masses of these quasiparticles should be deduced from nonperturbative calculations taking into account hard field modes, e.g., they can be associated with pole masses deduced from lattice QCD calculations. At the same time, the soft quantum fields are characterized by very high occupation numbers per mode. Therefore, to leading order, they can be well approximated by soft classical fields. This is precisely the picture we are going to utilize: massive quantum quasiparticles (hard modes) interacting via classical color fields. Our approach differs from that of Ref. [14] by a quantum treatment to quasiparticles instead of the classical one, and additionally by a relativistic description of the kinetic energy instead of the nonrelativistic approximation of Ref. [14].

## 2 Color Path Integrals

We consider a multi-component QGP consisting of  $N$  color quasiparticles:  $N_g$  gluons,  $N_q$  quarks and  $\bar{N}_q$  antiquarks. The Hamiltonian of this system is  $\hat{H} = \hat{K} + \hat{U}^C$ , consisting of kinetic and color Coulomb interaction parts

$$\hat{K} = \sum_i \sqrt{\hat{\mathbf{p}}_i^2 + m_i^2(T, \mu_q)}, \quad \hat{U}^C = \frac{1}{2} \sum_{i \neq j} \frac{g^2(T, \mu_q)(Q_i \cdot Q_j)}{4\pi|\mathbf{r}_i - \mathbf{r}_j|}. \quad (1)$$

Here the  $i$  and  $j$  summations run over all quark and gluon quasiparticles,  $i, j = 1, \dots, N$ , with  $N = N_q + \bar{N}_q + N_g$ , where  $N_q = N_u + N_d + N_s$  and  $\bar{N}_q = \bar{N}_u + \bar{N}_d + \bar{N}_s$  are the total numbers of quarks and antiquarks of all included flavours (*up*, *down* and *strange*), respectively. Further,  $\mathbf{r}_i$  are 3D vectors of the quasiparticle spatial coordinates, whereas  $Q_i$  denote Wong's quasiparticle color variable [8D-vectors in the  $SU(3)$  group], and  $(Q_i \cdot Q_j)$  denotes the scalar product of two color vectors. For the potential energy the non-relativistic approximation is used whereas for the kinetic energy the full relativistic form is retained, since the quasiparticle masses are not negligible compared to temperature. The eigenvalue equation of this Hamiltonian (the ‘‘spinless Salpeter equation’’) may be regarded as a well-defined approximation to the Bethe-Salpeter formalism [23–26] for the description of bound states within relativistic quantum field theory.

Thermodynamic properties in the grand canonical ensemble with a given inverse temperature  $\beta = 1/T$ , net-quark and strange chemical potentials  $\mu_q$  and  $\mu_s$  and fixed volume  $V$  are fully described by the grand partition function

$$Z(\mu_q, \mu_s, \beta, V) = \sum_{\{N\}} \frac{e^{\beta\mu_q(N_q - \bar{N}_q)} e^{\beta\mu_s(N_s - \bar{N}_s)}}{N_u! N_d! N_s! \bar{N}_u! \bar{N}_d! \bar{N}_s! N_g!} Z(\{N\}, V, \beta), \quad (2)$$

$$Z(\{N\}, V, \beta) = \sum_{\sigma} \int_V dr d\mu Q \rho(r, Q, \sigma; \{N\}; \beta), \quad (3)$$

where the variables  $\{N\} = \{N_u, N_d, N_s, \bar{N}_u, \bar{N}_d, \bar{N}_s, N_g\}$  are independent and  $\rho(r, Q, \sigma; \{N\}; \beta)$  denotes the diagonal matrix elements of the density operator  $\hat{\rho} = \exp(-\beta\hat{H})$ . Here  $r$ ,  $\sigma$  and  $Q$  denote the multi-dimensional vectors related to spatial, spin and color degrees of freedom, respectively, of all quarks, antiquarks and gluons. The  $\sigma$  summation and the spatial ( $dr \equiv d^3r_1 \dots d^3r_N$ ) and color ( $d\mu Q \equiv d\mu Q_1 \dots d\mu Q_N$ ) integrations run over all individual degrees of freedom of the quasiparticles, whereas  $d\mu Q_i$  denotes integration over the  $SU(3)$  group Haar measure [19]. In Eq. (2) we explicitly wrote a sum over different quark flavors (u,d,s) and assume that the strange chemical potential,  $\mu_s = -\mu_q$  (nonstrange matter). Since the masses and the coupling constant depend on temperature and on the quark chemical potential, all thermodynamic functions should be calculated through the respective derivatives of the logarithm of the partition function.

The (unknown) exact density operator  $\hat{\rho} = e^{-\beta\hat{H}}$  of interacting quantum systems can be constructed using a path integral approach based on the operator identity  $e^{-\beta\hat{H}} = e^{-\Delta\beta\hat{H}} \cdot e^{-\Delta\beta\hat{H}} \dots e^{-\Delta\beta\hat{H}}$ , where the r.h.s. contains  $n + 1$  identical factors with  $\Delta\beta = \beta/(n + 1)$ . The main advantage of this identity is that it allows us to use perturbation theory to obtain an approximation for each of the factors, which is applicable due to the smallness?? *large value* of the temperature  $1/\Delta\beta$ . Each factor should be calculated with an accuracy of the order of  $1/(n + 1)^\theta$ , with  $\theta > 1$ , as in this case the error of the whole product, in the limit of  $n \rightarrow \infty$ , will be equal to zero. Generalizing the electrodynamic plasma results [4] to the quark-gluon plasma case (see table 1), we may use the approximation<sup>1</sup>

$$\rho = e^{-\beta U} \frac{\text{per} \|\tilde{\phi}^{(n),(0)}\|_{N_g}}{\tilde{\lambda}_g^{3N_g}} \frac{\det \|\tilde{\phi}^{(n),(0)}\|_{N_q}}{\tilde{\lambda}_q^{3N_q}} \frac{\det \|\tilde{\phi}^{(n),(0)}\|_{N_{\bar{q}}}}{\tilde{\lambda}_{\bar{q}}^{3N_{\bar{q}}}} \prod_{l=1}^n \prod_{i=1}^N \phi_{ii}^{(l)}, \quad (4)$$

<sup>1</sup> For the sake of notational convenience, we ascribe the superscript <sup>(0)</sup> to the original variables.

where the proper (anti-)symmetrization for gluons (quarks/antiquarks) results in the permanents (determinants) in Eq. (4) while the effective total color Coulomb interaction energy

$$U = \frac{1}{n+1} \sum_{l=1}^{n+1} \frac{1}{2} \sum_{i,j(i \neq j)}^N \frac{\Delta\beta}{2} \left[ \Phi^{ij} \left( x_{ij}^{(l-1)}, x_{ij}^{(l-1)}, Q_i^{(0)}, Q_j^{(0)} \right) + \Phi^{ij} \left( x_{ij}^{(l)}, x_{ij}^{(l)}, Q_i^{(0)}, Q_j^{(0)} \right) \right] \quad (5)$$

is described in terms of the two-particle effective quantum Kelbg color potential [4, 11]

$$\Phi^{ij} \left( x_{ij}^{(l)}, x_{ij}^{(l)}, Q_i, Q_j, \Delta\beta \right) = \frac{g^2(T, \mu_q) \langle Q_i | Q_j \rangle}{4\pi |r_i^{(l)} - r_j^{(l)}|} \Phi \left( x_{ij}^{(l)} \right), \quad (6)$$

with  $x_{ij}^{(l)} = |r_i^{(l)} - r_j^{(l)}| / \Delta\lambda_{ij}$ ,  $\Delta\lambda_{ij} = \sqrt{2\pi\Delta\beta/m_{ij}}$ ,  $m_{ij} = m_i m_j / (m_i + m_j)$  and  $\Phi(x) = 1 - e^{-x^2} + \sqrt{\pi}x [1 - \text{erf}(x)]$ . The remaining quantities in Eq. (4) are defined as follows:  $\tilde{\lambda}_a^3 = \lambda_a^3 \sqrt{0.5\pi/(\beta m)^5}$  with  $\lambda_a = \sqrt{2\pi\beta/m_a}$  being the thermal wavelength of a quasiparticle of type ‘‘a’’ ( $a = q, \bar{q}, g$ ).

Here we have introduced the functions  $\phi_{ii}^{(l)} \equiv K_2(z_i^{(l)}) / (z_i^{(l)})^2$ , involving modified Bessel functions  $K_2$ , where  $z_i^{(l)} = \Delta\beta m_i(T, \mu_q) \sqrt{1 + |\xi_i^{(l)}|^2 / \Delta\beta^2}$ . The gluon matrix elements in the permanents are  $\phi_{i,j}^{(n),(0)} = K_2(z_{i,j}^{(n),(0)}) / (z_{i,j}^{(n),(0)})^2 \delta_\epsilon(Q_i^{(0)} - Q_j^{(0)})$ , while the quark and antiquark matrix elements entering the determinants are given by  $\tilde{\phi}_{i,j}^{(n),(0)} = K_2(z_{i,j}^{(n),(0)}) / (z_{i,j}^{(n),(0)})^2 \delta_\epsilon(Q_i^{(0)} - Q_j^{(0)}) \delta_{f_i, f_j} \delta_{\sigma_i, \sigma_j}$  and depend additionally on the spin variables  $\sigma_i$  and the flavor index  $f_i$  of the particle, which can take the values ‘‘up’’, ‘‘down’’ and ‘‘strange’’.  $\delta_\epsilon$  is a broadened delta function of the color vectors whereas the Kronecker symbols properly restrict Pauli blocking to particles with the identical spins and flavors. Also, we denoted  $z_{i,j}^{(n),(0)} = \Delta\beta m_i(T, \mu_q) \sqrt{1 + |r_i^{(0)} - r_j^{(n)}|^2 / \Delta\beta^2}$ . The coordinates of the quasiparticle ‘‘beads’’  $r_i^{(l)} = r_i^{(0)} + y_i^{(l)}$ , ( $l > 0$ ) are expressed in terms of  $r_i^{(0)}$  and vectors between neighboring beads of an  $i$  particle, defined as  $y_i^{(l)} = \sum_{k=1}^l \xi_i^{(k)}$ , while  $\xi_i^{(1)}, \dots, \xi_i^{(n)}$  are vector variable of integration at multiplication of the coordinate representation of mentioned above operator identity.

In the limit  $n \rightarrow \infty$  the functions  $\phi_{ii}^{(l)}$  describe the *relativistic measure* of the color path integrals [12, 13]. This measure is created by the *relativistic kinetic energy operator*  $K = \sqrt{p^2 + m^2(T, \mu_q)}$  and, in the limit of large particle mass, coincides with the Gaussian measure used in Feynman’s and Wiener’s path integrals (see table 1).

### 3 Color PIMC thermodynamic simulations of the QGP

Ideally the parameters of the model should be deduced from the QCD lattice data. However, presently this task is still quite ambiguous. Therefore, in the present simulations we take only one possible set of parameters and extend the analytical statements that are known for high temperatures to the lower temperatures of interest for the present analysis. The HTL perturbative values of  $m_g$  and  $m_q$  are known and given for  $T \gg T_c$  by [27]

$$m_g^2(\{\mu_q\}, T) = \frac{1}{12} \left( (2N_c + N_f)T^2 + \frac{3}{\pi^2} \sum_{q=u,d,s} \mu_q^2 \right) g^2(\{\mu_q\}), \quad (7)$$

$$m_q^2(\{\mu_q\}, T) = \frac{N_g}{16N_c} \left( T^2 + \frac{\mu_q^2}{\pi^2} \right) g^2(\{\mu_q\}), \quad (8)$$

where  $N_f$  is the number of quark flavors that can be excited,  $N_c = 3$  for the SU(3) group, and  $g$  is the QCD running coupling constant, generally depending on  $T$  and all  $\mu_q$ . According to Eqs. (7, 8) the masses do not depend on  $T$  and  $\mu_q$  separately but on their combinations  $z_g = \left( T^2 + \frac{3}{\pi^2(2N_c + N_f)} \sum_{q=u,d,s} \mu_q^2 \right)^{1/2}$  and  $z_q = \left( T^2 + \frac{\mu_q^2}{\pi^2} \right)^{1/2}$ , respectively. It is also reasonable to assume that  $g^2$  is a function of this single variable  $z_g$ . This choice is done because  $g^2$  (like the gluons) is related to the whole system rather than to one specific quark flavor.

Then we can use the same “one-loop analytic coupling” [28,29]

$$\alpha_s(Q^2) = \frac{4\pi}{11 - (2/3)N_f} \left[ \frac{1}{\ln(Q^2/\Lambda_{QCD}^2)} + \frac{\Lambda_{QCD}^2}{\Lambda_{QCD}^2 - Q^2} \right], \quad (9)$$

and use in our simulations  $2\pi z_g$  for  $Q$ . This coupling constant  $\alpha_s(z_g) = g^2/(4\pi)$  is displayed in the left panel of Fig. 1. To obtain model input formulas for the masses  $m_g$  and  $m_q$  we use the related dependencies from our paper [12] where we replace the temperature  $T$  by the expressions for  $z_g$  ( $z_q$ ) written above. The final dependencies are presented by Fig. 1 (right panel).

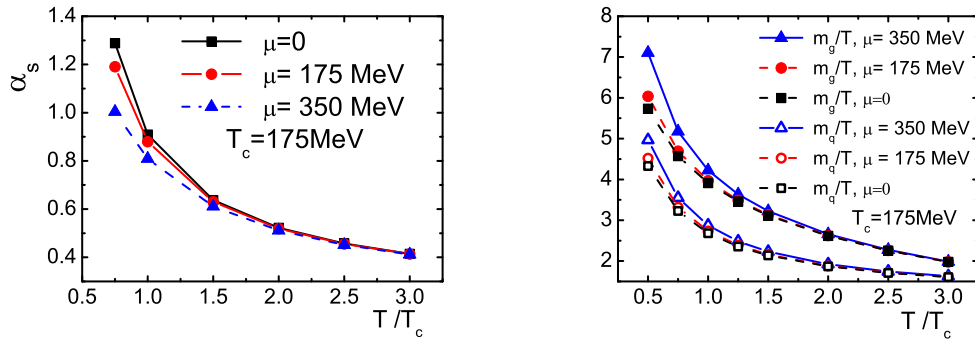


**Fig. 1** Temperature dependences of the model input quantities. **Left:** coupling constant  $\alpha_s$ . **Right:** quasiparticle mass-to-temperature ratio ( $m_q = m_{\bar{q}}$ ).

From Fig. 2 (upper left panel) it follows that the lattice QCD and color PIMC equations of state (EOS) of the QGP agree well for zero chemical potential. Similarly, good agreement of the lattice QCD Taylor expansion technique [30] and color PIMC EOS (blue area for  $\mu = 175$  MeV) is observed at non-zero chemical potential [13]. Interesting is also the behavior of pressure versus inverse density (specific volume, top right part of Fig. 2) and of the inverse density versus temperature (bottom left panel). At high temperatures our color PIMC results are close to the ideal Stefan–Boltzmann. However, at lower temperature, the influence of interactions is growing and results in a sharp pressure decrease whereas the quark density changes only weakly. An analogous behavior is observed in a dense electron-ion plasma and is connected with the formation of atomic and molecular bound states [4, 32]. The same is observed in electron–hole plasmas in semiconductors (formation of excitons and bi-excitons [31, 33]). The physical origin of the analogous behavior in the present QGP is, thus, the strong quasiparticle interaction which may give rise to the formation of bound states. In fact, we observe evidence of gluon–gluon interaction which may give rise to the formation of bound states. In fact, we observe evidence of gluon–gluon bound states and gluon balls at low temperatures, which can be seen in our gluon–gluon quasiparticle pair distribution functions (PDF  $g(r)$ )—the probability to find a particle pair at distance  $r$ ) at low temperatures (bottom right panel of Fig. 2). While in a non-interacting (ideal) classical system,  $g_{ab}(R) \equiv 1$ , interactions and quantum statistics result in a redistribution of the particles. The PDF in Fig. 2 are averaged over the quasiparticle colors. The maximum of  $r^2 g(r)$  at small interparticle distances supports the interpretation in terms of gluon bound states [31] which explains the observed behavior of pressure and density. At the same time, the quark–quark and quark–gluon PDF do not exhibit such peaks and are close to an ideal PDF.

To summarize, in this paper we demonstrated that color quantum Monte-Carlo simulations based on the quasiparticle model of the QGP are able to reproduce the lattice equation of state at zero and non-zero quark chemical potential at realistic model parameters (quasiparticle masses and coupling constant) even near and below the critical temperature. Moreover, our color PIMC simulations yield valuable insight into the internal structure of the QGP. Our results indicate that the QGP exhibits *quantum liquid-like* properties where the equation of state, quark density and pair distribution functions clearly reflect the existence of gluon-gluon bound states (glue balls), at temperatures just below the phase transition, while meson-like  $q\bar{q}$  bound states are not found.

We acknowledge stimulating discussions with G. Kalman, P. Levai, D. Blaschke, R. Bock and H. Stoecker.

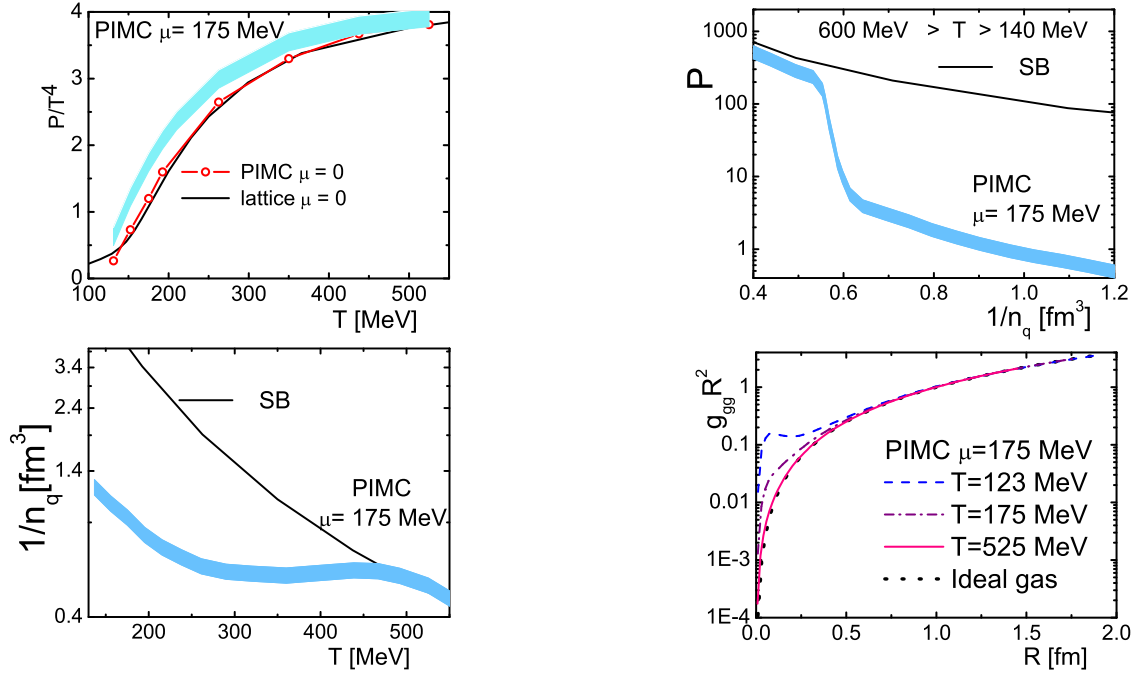


**Fig. 2** Thermodynamic properties of the quark-gluon plasma, **Top left:** Color PIMC (symbols) and lattice QCD (black line) [8] equation of state for  $\mu = 0$ , compared to the present color PIMC results for  $\mu = 175$  MeV (blue area). **Top right:** Stefan–Boltzmann (SB, black line) and PIMC pressure (blue) versus inverse quark density for  $\mu = 175$  MeV. **Bottom left:** Inverse quark density versus temperature for  $\mu = 175$  MeV – comparison of Stefan–Boltzmann (SB, black line) limit and the present grand canonical color PIMC results (blue). **Bottom right:** PIMC gluon–gluon quasiparticle pair distributions for different temperatures at  $\mu = 175$  MeV.

## References

- [1] C. Fortmann, H. J. Lee, T. Döppner, R. W. Falcone, A. L. Kritcher, O. L. Landen, C. Niemann and S. H. Glenzer, *Contrib. Plasma Phys.* **52**, 186 (2012)
- [2] M. Bonitz, C. Henning, and D. Block, *Rep. Prog. Physics* **73**, 066501 (2010)
- [3] B. Militzer, and R. Pollock, *Phys. Rev. E* **61**, 3470 (2000)
- [4] V. S. Filinov, M. Bonitz, W. Ebeling, and V.E. Fortov, *Plasma Phys. Control. Fusion* **43**, 743 (2001)
- [5] E. V. Shuryak, *Prog. Part. Nucl.* **62**, 048 (2009)
- [6] J. Schukraft, *J. Phys. Conf. Ser.* **381**, 012011 (2012)
- [7] C. Shen, and U. Heinz, *Phys. Rev.* **C85**, 054902 (2012)
- [8] S. Borsanyi, G. Endrodi, Z. Fodor, A. Jakovac, S.D. Katz, S. Krieg, C. Ratti, K.K. Szabo, *JHEP* **1011**, 077 (2010)
- [9] M. Cheng *et al.*, *Phys. Rev.* **D81**, 054504 (2010)
- [10] V. S. Filinov, M. Bonitz, Y. B. Ivanov, V. V. Skokov, P. R. Levashov, and V. E. Fortov, *Contrib. Plasma Phys.* **51**, 322 (2011) *ibid.* **52**, 135 (2012)
- [11] V. S. Filinov, Y. B. Ivanov, M. Bonitz, P. R. Levashov, and V. E. Fortov, *Phys. Atom. Nucl.* **75**, 693 (2012)
- [12] V. S. Filinov, Yu. B. Ivanov, V. E. Fortov, M. Bonitz, and P. R. Levashov, *Phys. Rev. C* **87**, 035207 (2013)
- [13] More details of the model are described in V.S. Filinov, M. Bonitz, Yu.B. Ivanov, M. Ilgenfritz, and V.E. Fortov, submitted to *Plasma Phys. Control. Fusion* (2014).
- [14] B. A. Gelman, E. V. Shuryak, and I. Zahed, *Phys. Rev. C* **74**, 044908 (2006)
- [15] P. Petreczky, F. Karsch, E. Laermann, S. Stickan, and I. Wetzorke, *Nucl. Phys. Proc. Suppl.* **109**, 513 (2002)
- [16] J. Liao, and E. V. Shuryak, *Phys. Rev. D* **73**, 014509 (2006)
- [17] F. Karsch, and M. Kitazawa, *Phys. Rev. D* **80**, 056001 (2009)
- [18] S. K. Wong, *Nuovo Cimento A* **65**, 689 (1970)
- [19] D. F. Litim, and C. Manue, *Phys. Rev. Lett.* **82**, 4981 (1999); *Nucl.Phys.* **B562**, 237 (1999); *Phys. Rev.* **D61**, 125004 (2000); *Phys. Rep.* **364**, 451 (2002)
- [20] R. D. Pisarski, *Phys. Rev. Lett.* **63**, 1129 (1989)
- [21] E. Braaten, and R. D. Pisarski, *Nucl. Phys* **B337**, 569 (1990); *ibid.* **B339**, 310 (1990)

- [22] J. Blaizot, and E. Iancu, *Phys. Rept.* **359**, 355 (2002)
- [23] E. E. Salpeter, and H. A. Bethe, *Phys. Rev.* **84**, 1232 (1951)
- [24] E. E. Salpeter, *Phys. Rev.* **87**, 328 (1952)
- [25] W. Lucha, F. F. Schoberl, and D. Gromes, *Phys. Rep.* **200**, 127 (1991);
- [26] W. Lucha, F. F. Schoberl, *Int. J. Mod. Phys. A* **7**, 6431 (1992)
- [27] M. Le Bellac, *Thermal Field Theory* (Cambridge University Press, Cambridge 1996)
- [28] D. V. Shirkov, and I. L. Solovtsov, *Phys. Rev. Lett.* **79**, 1209 (1997); *Nucl. Phys. Proc. Suppl.* **64**, 106 (1998)
- [29] G. M. Prospero, M. Raciti, and C. Simolo, *Prog. Part. Nucl. Phys.* **58**, 387 (2007)
- [30] S. Borsanyi, G. Endrodi, Z. Fodor, S. D. Katz, S. Krieg, C. Ratti, K. K. Szabo, *JHEP* **08**, 053 (2012)
- [31] V. S. Filinov, H. Fehske, M. Bonitz, V. E. Fortov, and P. R. Levashov, *Phys. Rev. E* **75**, 036401 (2007)
- [32] V. S. Filinov, V. E. Fortov, M. Bonitz, and D. Kremp, *Physics Lett. A* **274**, 228 (2000)
- [33] J. Schlee, A. Filinov, M. Bonitz, and H. Fehske, *Contrib. to Plasma Phys.* **52**, 819 (2012)